Hyperfine structure of $^2\Sigma$ molecules containing alkaline-earth-metal atoms

Jesus Aldegunde[1] and Jeremy M. Hutson[2,*]

[1]*Departamento de Quimica Fisica, Universidad de Salamanca, 37008 Salamanca, Spain*

[2]*Joint Quantum Centre (JQC) Durham-Newcastle, Department of Chemistry, Durham University, South Road, Durham, DH1 3LE, United Kingdom*

(Received 26 November 2017; published 17 April 2018)

Ultracold molecules with both electron spin and an electric dipole moment offer new possibilities in quantum science. We use density-functional theory to calculate hyperfine coupling constants for a selection of molecules important in this area, including RbSr, LiYb, RbYb, CaF, and SrF. We find substantial hyperfine coupling constants for the fermionic isotopes of the alkaline-earth-metal and Yb atoms. We discuss the hyperfine level patterns and Zeeman splittings expected for these molecules. The results will be important both to experiments aimed at forming ultracold open-shell molecules and to their applications.

DOI: 10.1103/PhysRevA.97.042505

There have recently been major advances in producing molecules in ultracold gases of alkali-metal atoms. Ultracold molecules have been produced from most combinations of alkali-metal atoms by magnetoassociation, in which pairs of atoms are converted into molecules by tuning a magnetic field adiabatically across a zero-energy Feshbach resonance. These "Feshbach molecules" are typically bound by less than $h \times 10$ MHz, which is less than part in 10^7 of the singlet well depth, and have very large internuclear separations. A few different molecules (^{40}K^{87}Rb [1], ^{87}Rb^{133}Cs [2,3], ^{23}Na^{40}K [4] and ^{23}Na^{87}Rb [5]) have recently been transferred from these long-range states to the absolute ground state by stimulated Raman adiabatic passage (STIRAP). These ground-state molecules have significant electric dipole moments, and hold great promise for studying ultracold dipolar matter, for precision measurement, and for applications in quantum science and technology.

The alkali-metal dimers all have singlet ground states, with no net electron spin. This limits their tunability with magnetic fields. There is now great interest in producing ultracold molecules with electron spin as well as an electric dipole. Such molecules could be used to create new types of quantum many-body systems [6,7]. Promising candidates include molecules formed from an alkali-metal atom and a laser-coolable closed-shell atom such as Yb or Sr. Żuchowski *et al.* [8] showed that magnetically tunable Feshbach resonances can exist in such systems, mediated by the dependence of the alkali-metal hyperfine coupling on the internuclear distance. Brue and Hutson [9] carried out a detailed theoretical study of such resonances in alkali metal + Yb systems. Brue and Hutson [10] also identified a different mechanism that can cause additional resonances in systems containing closed-shell atoms with nuclear spin (which are all fermionic for Sr and Yb), mediated in this case by hyperfine coupling involving the Sr or Yb nucleus. The first Feshbach resonances of both these types have recently been observed in RbSr [11], along with resonances due to another mechanism involving the tensorial coupling between the electron and nuclear spins. It is likely that ultracold ground-state $^2\Sigma$ molecules of this type will be produced within the next few years.

In parallel with the work on producing ultracold molecules from atoms, there have been major advances in direct laser-cooling of molecules such as CaF and SrF, which also have $^2\Sigma$ ground states. Barry *et al.* [12] have cooled SrF to about 2.5 mK in a magneto-optical trap (MOT), and Truppe *et al.* [13] have achieved sub-Doppler cooling of CaF in a blue-detuned MOT to about 50 μK.

Although the basic spectroscopy of molecules in $^2\Sigma$ states is well understood [14], little is known quantitatively about the fine and hyperfine coupling constants of molecules formed from alkali-metal atoms and closed-shell atoms, or about isotopologs of CaF and SrF containing metal atoms with nonzero spin. The magnitudes of the coupling constants will have profound effects on the patterns of energy levels for ground-state molecules, and on how the levels cross and avoided-cross one another in magnetic, electric, and laser fields. This will in turn affect the possibilities for state transfer and quantum control. The coupling constants are also important to understand the strengths of Feshbach resonances [8–11]. In this paper we present calculations of the fine and hyperfine constants for RbSr, LiYb, RbYb, CaF, and SrF, using density-functional theory, which allow these effects to be explored.

I. MOLECULAR HAMILTONIAN

The effective Hamiltonian for a $^2\Sigma$ diatomic molecule can be written

$$H_{\rm eff} = H_{\rm rfs} + H_{\rm hfs} + H_{\rm S} + H_{\rm Z}, \tag{1}$$

where the four contributions correspond to the rotational plus fine-structure, hyperfine-structure, Stark, and Zeeman Hamiltonians, respectively.

The rotational plus fine-structure Hamiltonian $H_{\rm rfs}$ takes the standard form

$$H_{\rm rfs} = B_v \boldsymbol{N}^2 - D_v \boldsymbol{N}^2 \boldsymbol{N}^2 + \gamma \boldsymbol{S} \cdot \boldsymbol{N}, \tag{2}$$

*J.M.Hutson@durham.ac.uk

where $\boldsymbol{N}$ is the angular momentum for rotation of the molecule about its center of mass and $\boldsymbol{S}$ is the electron spin. The third term in Eq. (2) represents the electron spin-rotation interaction. The hyperfine Hamiltonian $H_{\rm hfs}$ may be written

$$H_{\rm hfs} = \sum_{i=1}^{2} e\boldsymbol{Q}_i \cdot \boldsymbol{q}_i + \sum_{i=1}^{2} \boldsymbol{S} \cdot \boldsymbol{A}_i \cdot \boldsymbol{I}_i, \tag{3}$$

where $\boldsymbol{I}_1$ and $\boldsymbol{I}_2$ are the spins of nuclei 1 and 2. The first term here represents the interaction between the quadrupole tensor $e\boldsymbol{Q}_i$ of nucleus i and the electric field gradient tensor $\boldsymbol{q}_i$ at the nucleus due to the electrons; it is commonly written in terms of a scalar nuclear quadrupole coupling constant $(eQq)_i$. The second term represents the interaction between the electron and nuclear spins. It is usual to separate the isotropic and anisotropic components of the hyperfine tensor $\boldsymbol{A}_i$ [15],

$$b_{\rm F} = A_{\rm iso} = \frac{A_\parallel + 2A_\perp}{3} \quad \text{and} \quad t = A_{\rm dip} = \frac{A_\parallel - A_\perp}{3}, \tag{4}$$

so that

$$\boldsymbol{S} \cdot \boldsymbol{A}_i \cdot \boldsymbol{I}_i = b_{{\rm F},i} \boldsymbol{S} \cdot \boldsymbol{I}_i + t_i \sqrt{6}\, T^2(\boldsymbol{S}, \boldsymbol{I}_i) \cdot T^2(C), \tag{5}$$

where T^2 indicates a spherical tensor of rank 2. $T^2(C)$ has components $C^2_q(\theta,\phi)$, where C is a renormalized spherical harmonic and θ,ϕ are the polar coordinates of the internuclear vector. The isotropic (scalar) component $b_{{\rm F},i}$ arises from the Fermi contact interaction, whereas the anisotropic component t_i arises from dipolar interactions. The notation involving γ, $(eQq)_i$, $b_{{\rm F},i}$, and t_i coincides with that employed by Brown and Carrington [14] (see, for example, page 607), where explicit expressions for the matrix elements in different basis sets can be found. The alternative constants of Frosch and Foley [16] are related to these by $c_i = 3t_i$ and $b_i = b_{{\rm F},i} - t_i$.

The effect of the external fields is described by $H_{\rm S}$ and $H_{\rm Z}$, which represent the Stark and Zeeman Hamiltonians. The Stark Hamiltonian is

$$H_{\rm S} = -\boldsymbol{\mu} \cdot \boldsymbol{E} - \tfrac{1}{2} \boldsymbol{E} \cdot \boldsymbol{\alpha} \cdot \boldsymbol{E}. \tag{6}$$

It includes both a linear term to describe the interaction of the molecular dipole $\boldsymbol{\mu}$ with a static electric field $\boldsymbol{E}$ and a quadratic term involving the molecular polarizability tensor $\boldsymbol{\alpha}$. The latter is usually small for static fields, but may be used with a frequency-dependent polarizability $\boldsymbol{\alpha}(\omega)$ to account for the ac Stark effect due to a nonresonant laser field [17]. The Zeeman Hamiltonian is

$$H_{\rm Z} = -g_\parallel \mu_{\rm B} \boldsymbol{S} \cdot \boldsymbol{B} + \Delta g_\perp \mu_{\rm B} [\boldsymbol{S} \cdot \boldsymbol{B} - (\boldsymbol{S} \cdot \hat{z})(\boldsymbol{B} \cdot \hat{z})]$$
$$- g_{\rm r} \mu_{\rm B} \boldsymbol{N} \cdot \boldsymbol{B} - \sum_{i=1}^{2} g_i \mu_{\rm N} \boldsymbol{I}_i \cdot \boldsymbol{B}(1 - \sigma_i). \tag{7}$$

The first term describes the isotropic part of the interaction of the electron spin with an external magnetic field $\boldsymbol{B}$; $g_\parallel \approx g_e \approx -2.0023$ is the electron g factor parallel to the molecular axis $\hat{z}$ and $\mu_{\rm B}$ is the Bohr magneton. The second term is an anisotropic correction; $\Delta g_\perp = g_\parallel - g_\perp$, where $g_\perp$ is the electron g factor perpendicular to the molecular axis (defined to be negative, like g_e). The third and fourth terms describe the interaction of the molecular rotation and the nuclear spins with the magnetic field; $g_{\rm r}$ is the rotational g factor, and g_i and σ_i are the bare nuclear g factor and shielding factor for nucleus i. $\mu_{\rm N}$ is the nuclear magneton. The Zeeman Hamiltonian $H_{\rm Z}$ is dominated by the first term, but the remaining contributions cause small shifts that may have important consequences for resonance positions [11] and for the decoherence of molecules in magnetic traps [18].

The expressions given above neglect various small terms such as the interactions between the two nuclear spins and between the nuclear spins and molecular rotation. These terms can be important for closed-shell molecules [19–22], but for open-shell molecules they are less important because the terms involving electron spin are always present and are two or more orders of magnitude larger. A full description of the Hamiltonian, including the discarded terms, can be found in Ref. [14].

II. CALCULATION OF THE COUPLING CONSTANTS

Molecular fine-structure and hyperfine constants may in principle be calculated using either wave-function-based methods or density-functional theory (DFT). However, wave-function-based methods become very complex for hyperfine interactions in molecules containing heavy atoms, where very large basis sets are needed and relativistic effects are important. Calculations of potential curves for such molecules commonly use effective core potentials, but these are of doubtful accuracy for hyperfine interactions. We therefore choose to use DFT in the current work, and obtain values of the coupling constants (eQq), $b_{\rm F}$, t, and $\Delta g_\perp$ using the Amsterdam density functional (ADF) package [23,24]. The ADF package includes its own all-electron basis sets of Slater functions for all the elements of the periodic table and incorporates relativistic corrections.

In the present calculations, we employ all-electron quadruple-ζ basis sets with four polarization functions (QZ4P). Relativistic effects are included by means of the two-component zero-order regular approximation (ZORA) [25–27]. The electron spin-rotation coupling constant, γ, is obtained from the components of the $\boldsymbol{g}$ tensor [15] and the rotational constant using Curl's approximation [28,29]

$$\gamma = -2B\, \Delta g_\perp. \tag{8}$$

According to Weltner [30], Curl's formula is accurate to about $\pm 10\%$.

We have carried out both spin-restricted and unrestricted DFT calculations using the B3LYP [31] and PBE0 [32] functionals, for a variety of $^2\Sigma$ molecules for which experimental values are available. The full results of these tests for the magnetic fine and hyperfine coupling constants are given in the Appendix. We conclude that spin-restricted B3LYP calculations are the most reliable, and these results are summarized in Table I. The largest fractional discrepancies are mostly in cases where the constants concerned are small and thus play a minor role for the molecule in question. For the remaining molecules, the spin-restricted results for $\Delta g_\perp$ (or equivalently γ) are accurate to 30% or better, with the exceptions of GaO and InO. The agreement is significantly better for $b_{\rm F}$ and t, except for InO. The exceptions probably arise because the ground states of these oxide radicals are mixtures of two electronic configurations with similar energies [33]. Magnetic properties are very sensitive to the balance between the configurations.

TABLE I. Comparison between experimental and theoretical values of $\Delta g_\perp$, γ, b_F, and t for $^2\Sigma$ molecules, computed through restricted DFT calculations using the B3LYP [31] functional. Asterisks indicate cases where the signs of the components of the $\boldsymbol{A}$ tensor were not reported in the experimental papers and have been assigned to match the theoretical results [36]. The acronyms GP, NM, and AM stand for gas phase, neon matrix, and argon matrix, respectively, and refer to the conditions used to record the spectra. Experimental results labeled CA are obtained by applying Curl's approximation to $\Delta g_\perp$ or γ, depending on the case. Theoretical values of γ are always obtained from $\Delta g_\perp$ using Curl's approximation.

Molecule (MX)	Source	$\Delta g_\perp$	γ (MHz)	$b_{F,M}$ (MHz)	t_M (MHz)	$b_{F,X}$ (MHz)	t_X (MHz)
^{103}Rh^{13}C	Expt. [37] (NM)	0.0518(6)		−1097(1)	−8(1)	66(1)	11(1)
	Expt. [38] (GP)		−1861(6)				
	B3LYP-R	0.0572	−1930	−1010	−2.5	59.3	8.5
^{11}B^{17}O	Expt. [39] (NM)	−0.0017(3)	$1.8(3) \times 10^2$ (CA)	1033(1)	25(1)	−19(3)	−12(3)
	B3LYP-R	−0.0025	2.61×10^2	873	31.1	−17.0	−16.6
^{11}B^{33}S	Expt. [40] (NM)	−0.0081(1)		795.6(3)	28.9(3)		
	Expt. [40,41] (GP)		$3.8(6) \times 10^2$				
	B3LYP-R	−0.0116	5.46×10^2	620	35.3	13.8	18.7
^{27}Al^{17}O	Expt. [33] (NM)	−0.0012(2)		766(1)	52(1)	2(1)	−50(1)
	Expt. [42] (GP)		51.66(4)	738(1)	56.39(8)		
	B3LYP-R	0.0017	−62.4	714	58.1	−3.9	−46.4
^{69}Ga^{17}O	Expt. [33] (NM)	−0.0343(2)	854(5) (CA)	1483(1)	127(1)	8(1)	−77(1)
	B3LYP-R	−0.0622	1550	1650	139	13.2	−81.4
^{115}In^{17}O	Expt. [33] (NM)	−0.192(2)	$3.06(3) \times 10^3$ (CA)	1368(2)	180(1)	35(1)	−131(1)
	B3LYP-R	−0.337	5.38×10^3	2300	170	75.3	−153
^{45}Sc^{17}O	Expt. [43] (NM)	−0.0005(3)	14(9) (CA)	2018(1)	24.7(4)	−20.3(3)	0.4(2)
	B3LYP-R	−0.0001	3.0	1850	13.5	−22.9	−0.3
^{89}Y^{17}O	Expt. [43] (NM)	−0.0002(1)		–807.5(4)	–9.5(3)	−16.8(2)	0.0(2)
	Expt. [44] (GP)		−9.2254(1)	−762.976(2)	−9.449(1)		
	B3LYP-R	−0.0005	11.4	−750	−5.2	−19.2	−0.3
^{139}La^{17}O	Expt. [43] (NM)	−0.003(2)		3751(5)	29(4)	Abs.val.<10	
	Expt. [45] (GP)		66.1972(5)	3631.9(1)	31.472(1)		
	B3LYP-R	−0.0046	91.3	3460	16.6	−12.5	−0.6
^{67}Zn^{1}H	Expt. [46] (NM)	−0.0182(3)	$7.2(1) \times 10^3$ (CA)	630(1)	15(1)	503(1)	−1(1)
	B3LYP-R	−0.0244	9.79×10^3	616	23.8	382	1.4
^{67}Zn^{19}F	Expt. [47] (NM)	−0.006(1)	$1.3(2) \times 10^2$ (CA)			319(2)	177(2)
	B3LYP-R	−0.0073	1.59×10^2	1160	15.4	266	210
^{111}Cd^{19}F	Expt. [47] (NM)	−0.017(2)	$4.8(6) \times 10^2$ (CA)			266(3)	202(2)
	B3LYP-R	−0.0314	8.79×10^2	−3600	−255	567	229
^{67}Zn^{107}Ag	Expt. [48] (AM)	−0.0118(2)	39(1) (CA)			−1324(3)*	0(1)
	B3LYP-R	−0.0158	52.0	306	6.9	−1250	−0.6
^{105}Pd^{1}H	Expt. [49] (AM)	0.291(1)	$-1.252(4) \times 10^5$ (CA)	−823(4)	−22(3)		
	Expt. [49] (NM)	0.291(1)	$-1.252(4) \times 10^5$ (CA)	−857(4)	−16(3)		
	B3LYP-R	0.266	-1.14×10^5	−914	−2.4	117	7.0
^{111}Cd^{1}H	Expt. [50] (GP)	−0.0567(2) (CA)	$1.811(6) \times 10^4$	−3764(26)	−122(6)	558(10)	
	Expt. [51] (GP)			−3766.3(15)	−143(1)	549.8(18)	−2.4(8)
	B3LYP-R	−0.0735	2.4×10^4	−3920	−175	374	0.9
^{111}Cd^{107}Ag	Expt. [48] (AM)	−0.0312(2)	68.9(4)	−2053(3)*	−63(3)*	−1327(3)*	0(1)
	B3LYP-R	−0.0400	88.4	−2010	−55.4	−1210	−0.6
^{7}Li^{40}Ca	Expt. [52] (GP)	−0.0068(1) (CA)	103(2)				
	B3LYP-R	−0.0119	179	218	0.2	−107	−4.6
^{7}Li^{138}Ba	Expt. [53] (GP)	−0.1205(1) (CA)	1384.5(9)				
	B3LYP-R	−0.129	1480	162	0.3	806	28.1
^{40}Ca^{19}F	Expt. [54] (GP)	−0.00193(1) (CA)	39.49793(2)			122.025(1)	13.549(1)
	B3LYP-R	−0.00180	37.2			127	8.0
^{88}Sr^{19}F	Expt. [55] (GP)	−0.00495(1) (CA)	74.79485(10)			107.1724(10)	10.089(10)
	B3LYP-R	−0.00463	69.9			112	6.8

The accuracy of B3LYP calculations for nuclear quadrupole coupling constants has been established previously [19,34,35].

The ADF program produces values of the coupling constants for a single isotopolog, usually the one containing the most abundant isotopes. Coupling constants for other isotopologs are obtained using simple scalings involving rotational constants, nuclear g factors and nuclear quadrupole moments.

TABLE II. Coupling constants for the isotopologs of RbSr, LiYb, RbYb, CaF, and SrF, obtained from spin-restricted B3LYP calculations.

AX	I_A	I_X	γ/MHz	$b_{F,A}$ (MHz)	t_A (MHz)	$b_{F,X}$ (MHz)	t_X (MHz)	$(eQq)_A$/MHz	$(eQq)_X$/MHz
^{85}Rb^{84}Sr	5/2	0	33.8	767	0.01			−7.5	
^{85}Rb^{86}Sr	5/2	0	33.4	767	0.01			−7.5	
^{85}Rb^{87}Sr	5/2	9/2	33.2	767	0.01	−65.2	−3.7	−7.5	−23.1
^{85}Rb^{88}Sr	5/2	0	33.0	767	0.01			−7.5	
^{87}Rb^{84}Sr	3/2	0	33.4	2600	0.04			−3.6	
^{87}Rb^{86}Sr	3/2	0	33.0	2600	0.04			−3.6	
^{87}Rb^{87}Sr	3/2	9/2	32.8	2600	0.04	−65.2	−3.7	−3.6	−23.1
^{87}Rb^{88}Sr	3/2	0	32.6	2600	0.04			−3.6	
^{6}Li^{168}Yb	1	0	1880	97.2	0.1			≈0	
^{6}Li^{170}Yb	1	0	1880	97.2	0.1			≈0	
^{6}Li^{171}Yb	1	1/2	1880	97.2	0.1	1440	83.1	≈0	
^{6}Li^{172}Yb	1	0	1880	97.2	0.1			≈0	
^{6}Li^{173}Yb	1	5/2	1880	97.2	0.1	−396	−22.9	≈0	−786
^{6}Li^{174}Yb	1	0	1880	97.2	0.1			≈0	
^{6}Li^{176}Yb	1	0	1880	97.2	0.1			≈0	
^{7}Li^{168}Yb	3/2	0	1620	257	0.2			0.1	
^{7}Li^{170}Yb	3/2	0	1620	257	0.2			0.1	
^{7}Li^{171}Yb	3/2	1/2	1620	257	0.2	1440	83.1	0.1	
^{7}Li^{172}Yb	3/2	0	1620	257	0.2			0.1	
^{7}Li^{173}Yb	3/2	5/2	1620	257	0.2	−396	−22.9	0.1	−786
^{7}Li^{174}Yb	3/2	0	1620	257	0.2			0.1	
^{7}Li^{176}Yb	3/2	0	1620	257	0.2			0.1	
^{85}Rb^{168}Yb	5/2	0	54.9	844	0.02			−5.1	
^{85}Rb^{170}Yb	5/2	0	54.7	844	0.02			−5.1	
^{85}Rb^{171}Yb	5/2	1/2	54.6	844	0.02	499	36.8	−5.1	
^{85}Rb^{172}Yb	5/2	0	54.5	844	0.02			−5.1	
^{85}Rb^{173}Yb	5/2	5/2	54.4	844	0.02	−137	−10.1	−5.1	−303
^{85}Rb^{174}Yb	5/2	0	54.3	844	0.02			−5.1	
^{85}Rb^{176}Yb	5/2	0	54.1	844	0.02			−5.1	
^{87}Rb^{168}Yb	3/2	0	54.1	2860	0.1			−2.3	
^{87}Rb^{170}Yb	3/2	0	53.9	2860	0.1			−2.3	
^{87}Rb^{171}Yb	3/2	1/2	53.7	2860	0.1	499	36.8	−2.3	
^{87}Rb^{172}Yb	3/2	0	53.6	2860	0.1			−2.3	
^{87}Rb^{173}Yb	3/2	5/2	53.5	2860	0.1	−137	−10.1	−2.3	−303
^{87}Rb^{174}Yb	3/2	0	53.4	2860	0.1			−2.3	
^{87}Rb^{176}Yb	3/2	0	53.2	2860	0.1			−2.3	
^{40}Ca^{19}F	0	1/2	37.2			127	8.0		
^{42}Ca^{19}F	0	1/2	36.6			127	8.0		
^{43}Ca^{19}F	7/2	1/2	36.3	−404	−3.0	127	8.0	9.9	
^{44}Ca^{19}F	0	1/2	36.1			127	8.0		
^{46}Ca^{19}F	0	1/2	35.6			127	8.0		
^{48}Ca^{19}F	0	1/2	35.2			127	8.0		
^{84}Sr^{19}F	0	1/2	70.5			112	6.8		
^{86}Sr^{19}F	0	1/2	70.2			112	6.8		
^{87}Sr^{19}F	9/2	1/2	70.1	−525	−3.8	112	6.8	−150	
^{88}Sr^{19}F	0	1/2	69.9			112	6.8		

III. COUPLING CONSTANTS FOR RbSr, LiYb, RbYb, CaF, AND SrF

Table II gives the coupling constants for all stable isotopologs of RbSr, LiYb, RbYb, CaF, and SrF, obtained from spin-restricted B3LYP calculations at the equilibrium geometries, $R_e = 4.67$ Å for RbSr [56], 3.52 Å for LiYb [9], 4.91 Å for RbYb [9], 1.95 Å for CaF [54], and 2.07 Å for SrF [57]. The spin-restricted results for one isotopolog of each molecule are compared with unrestricted results in Table III; the differences are mostly within 20%, although for LiYb some of them approach 30%.

Experimental results are available for CaF [54] and SrF [55], but only for isotopologs containing metal atoms with zero nuclear spin. The agreement between the experimental and theoretical results is good, with errors below 15% for CaF and SrF. The present results also agree with previous calculations of b_F as a function of internuclear distance for Rb in RbSr [8] and Rb in RbYb [9].

TABLE III. Coupling constants for one isotopolog of RbSr, LiYb, RbYb, CaF, and SrF calculated using restricted and unrestricted calculations.

AX	Source	I_A	I_X	γ/MHz	$b_{F,A}$ (MHz)	t_A (MHz)	$b_{F,X}$ (MHz)	t_X (MHz)	$(eQq)_A$/MHz	$(eQq)_X$/MHz
^{85}Rb^{87}Sr	B3LYP-R	5/2	9/2	33.2	767	0.01	−65.2	−3.7	−7.5	−23.1
	B3LYP-U	5/2	9/2	26.7	893	−0.50	−52.1	−3.8	−7.3	−23.3
^{7}Li^{173}Yb	B3LYP-R	3/2	5/2	1620	257	0.2	−396	−22.9	0.1	−786
	B3LYP-U	3/2	5/2	1190	364	0.2	−294	−20.5	0.1	−673
^{85}Rb^{173}Yb	B3LYP-R	5/2	5/2	54.4	844	0.02	−137	−10.1	−5.1	−303
	B3LYP-U	5/2	5/2	40.9	962	−0.16	−105	−9.0	−4.8	−257
^{43}Ca^{19}F	B3LYP-R	7/2	1/2	36.3	−404	−3.0	127	8.0	9.9	
	B3LYP-U	7/2	1/2	38.9	−443	−4.8	126	8.2	10.2	
^{87}Sr^{19}F	B3LYP-R	9/2	1/2	70.1	−525	−3.8	112	6.8	−150	
	B3LYP-U	9/2	1/2	65.2	−570	−6.0	114	7.0	−154	

In molecular spectroscopy, a $^2\Sigma$ molecule without nuclear spin is commonly described using Hund's case (b), in which the electron spin S couples to the molecular rotation N to form a resultant J. However, J is a useful quantum number only if the hyperfine interactions are weak compared to the spin-rotation interaction, which is not the case for most of the molecules considered here. In the present work we couple the electron and nuclear spins *before* coupling their vector sum to the molecular rotation.

There is some difficulty in choosing a notation for molecular quantum numbers that does not clash with usage in either atomic physics or molecular spectroscopy. In molecular spectroscopy, F is commonly used for the total angular momentum of a molecule, including rotation and all spins. However, in atomic physics, F is often used for the total angular momentum of a single atom. For collision problems and Van der Waals complexes, there is a well-established convention that quantum numbers that apply to individual colliding species (or monomers) are converted to lower case, reserving the upper-case letter for the corresponding quantum number of the collision complex [58]. We follow this convention here and retain s, i, and f for the electron spin, nuclear spin, and total angular momentum of individual atoms, and use F for the resultant of f_1 and f_2. In our notation, F is thus the total angular momentum of the molecule *excluding rotation*. This accords with usage in systems such as RbCs and Cs_2 [59,60], although Brown and Carrington [14] use G in this context. We use N for the mechanical rotation of the pair (equivalent to the partial-wave quantum number L in collisions). We designate the total angular momentum of the molecule $\mathcal{F}$, the resultant of F and N. All the quantum numbers can have projections denoted m_i, M_F, etc., which may be nearly conserved in certain field regimes.

Figure 1 shows the Zeeman splitting of the hyperfine levels for the lowest two rotational levels of ^{87}Rb^{88}Sr at magnetic fields up to 20 G. The hyperfine coupling constant $b_{F,Rb}$ is 2.60 GHz, which is reduced by about 25% from its atomic value of 3.42 GHz. The resulting splitting is 5.2 GHz, which is considerably larger than the rotational spacing of 1.1 GHz, so levels correlating with $f = 2$ are well off the top of Fig. 1. The rotationless $N = 0$ state, with $f = 1$ and $F = 1$, splits into three sublevels with projection M_F, just like a free ^{87}Rb atom. By contrast, the $N = 1$ state with $F = f = 1$ is split into three zero-field levels with $\mathcal{F} = 0$, 1, and 2 by the spin-rotation coupling. When a magnetic field is applied, each of these splits initially into $2\mathcal{F} + 1$ components labeled by the total projection $M_\mathcal{F}$. However, states of the same $M_\mathcal{F}$ originating from different $\mathcal{F}$ levels mix as the field increases; at higher fields, $\mathcal{F}$ is no longer a good quantum number and the magnetic sublevels are better described by M_F and M_N. In this regime, from 30 to about 1000 G, $F = f$ remains nearly conserved. At even higher fields, levels of different F will mix and eventually the best quantum numbers are $M_S = m_s$, $M_I = m_i$, and M_N.

The situation is more complicated when the closed-shell atom has nonzero nuclear spin. We consider briefly the example of ^{87}Rb^{87}Sr, which is topical because Feshbach resonances have recently been observed for this combination [11]. The largest coupling is still between S and i_{Rb} to form $f_{Rb} = 1$ and 2, but in this case $f_{Rb} = 1$ couples to $i_{Sr} = 9/2$ to

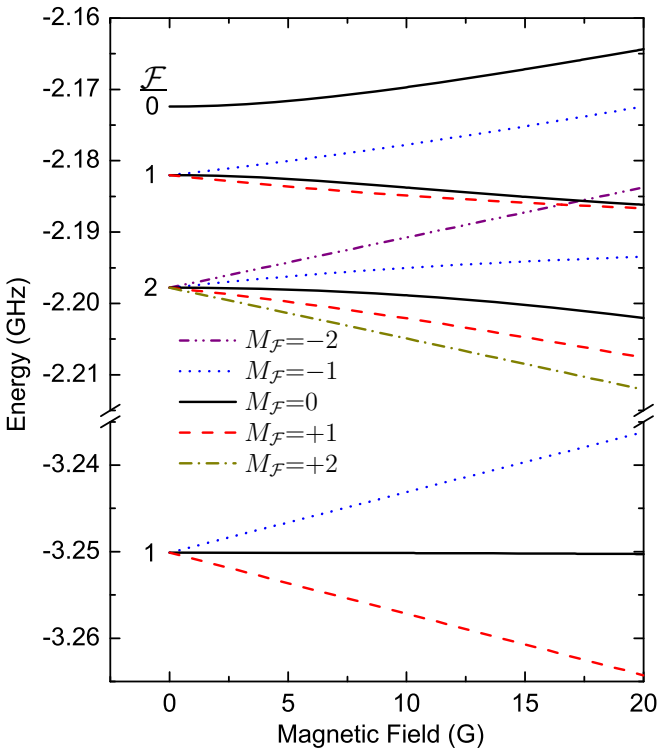

FIG. 1. Zeeman splitting of the lowest hyperfine energy levels of ^{87}Rb^{88}Sr for magnetic fields up to 20 G.

TABLE IV. Comparison between experimental and theoretical values of $\Delta g_\perp$, γ, b_F, and t for $^2\Sigma$ molecules computed through restricted (R) and unrestricted (U) DFT calculations using the B3LYP [31] and PBE0 [32] functionals. Notation is the same as in Table I.

Molecule (MX)	Source	$\Delta g_\perp$	γ (MHz)	$b_{F,M}$ (MHz)	t_M (MHz)	$b_{F,X}$ (MHz)	t_X (MHz)
$^{103}Rh^{13}C$	Expt. [37] (NM)	0.0518(6)		−1097(1)	−8(1)	66(1)	11(1)
	Expt. [38] (GP)		−1861(6)				
	B3LYP-U	0.0720	−2420	−1080	−6.7	60.0	13.5
	B3LYP-R	0.0572	−1930	−1010	−2.5	59.3	8.5
	PBE0-U	0.0799	−2690	−1080	−7.9	46.3	13.8
	PBE0-R	0.0625	−2100	−999	−2.8	55.2	8.4
$^{11}B^{17}O$	Expt. [39] (NM)	−0.0017(3)	$1.8(3)\times10^2$ (CA)	1033(1)	25(1)	−19(3)	−12(3)
	B3LYP-U	−0.0023	2.38×10^2	1080	29.1	−10.7	−21.5
	B3LYP-R	−0.0025	2.61×10^2	873	31.1	−17.0	−16.6
	PBE0-U	−0.0023	2.43×10^2	1040	26.9	−10.4	−23.3
	PBE0-R	−0.0024	2.55×10^2	829	30.2	−17.8	−16.6
$^{11}B^{33}S$	Expt. [40] (NM)	−0.0081(1)		795.6(3)	28.9(3)		
	Expt. [40,41] (GP)		$3.8(6)\times10^2$				
	B3LYP-U	−0.0102	4.80×10^2	824	34.0	2.3	22.1
	B3LYP-R	−0.0116	5.46×10^2	620	35.3	13.8	18.7
	PBE0-U	−0.0101	4.78×10^2	805	31.4	3.4	23.3
	PBE0-R	−0.0108	5.12×10^2	595	33.8	14.4	18.8
$^{27}Al^{17}O$	Expt. [33] (NM)	−0.0012(2)		766(1)	52(1)	2(1)	−50(1)
	Expt. [42] (GP)		51.66(4)	738(1)	56.39(8)		
	B3LYP-U	0.0007	−26.6	472	62.2	7.6	−64.8
	B3LYP-R	0.0017	−62.4	714	58.1	−3.9	−46.4
	PBE0-U	−0.0002	6.7	434	60.3	18.6	−61.9
	PBE0-R	0.0010	−35.1	687	56.1	−3.5	−43.9
$^{69}Ga^{17}O$	Expt. [33] (NM)	−0.0343(2)	854(5) (CA)	1483(1)	127(1)	8(1)	−77(1)
	B3LYP-U	−0.0387	965	635	142	12.3	−95.8
	B3LYP-R	−0.0622	1550	1650	139	13.2	−81.4
	PBE0-U	−0.0354	883	536	142	25.3	−93.1
	PBE0-R	−0.0561	1400	1670	139	11.1	−75.5
$^{115}In^{17}O$	Expt. [33] (NM)	−0.192(2)	$3.06(3)\times10^3$ (CA)	1368(2)	180(1)	35(1)	−131(1)
	B3LYP-U	−0.152	2.42×10^3	389	221	27.9	−125
	B3LYP-R	−0.337	5.38×10^3	2300	170	75.3	−153
	PBE0-U	−0.137	2.15×10^3	205	232	37.7	−120
	PBE0-R	−0.270	4.26×10^3	2390	194	59.5	−130
$^{45}Sc^{17}O$	Expt. [43] (NM)	−0.0005(3)	14(9) (CA)	2018(1)	24.7(4)	−20.3(3)	0.4(2)
	B3LYP-U	−0.0007	20.9	1990	22.1	−20.2	0.7
	B3LYP-R	−0.0001	3.0	1850	13.5	−22.9	−0.3
	PBE0-U	−0.0012	34.6	1830	22.1	−16.1	0.5
	PBE0-R	−0.0003	10.2	1690	13.1	−21.1	−0.3
$^{89}Y^{17}O$	Expt. [43] (NM)	−0.0002(1)		−807.5(4)	−9.5(3)	−16.8(2)	0.0(2)
	Expt. [44] (GP)		−9.2254(1)	−762.976(2)	−9.449(1)		
	B3LYP-U	−0.0004	8.7	−804	−8.0	−17.7	0.3
	B3LYP-R	−0.0005	11.4	−750	−5.2	−19.2	−0.3
	PBE0-U	−0.0013	28.7	−749	−8.1	−13.8	0.3
	PBE0-R	−0.0013	28.8	−695	−5.0	−17.6	−0.3
$^{139}La^{17}O$	Expt. [43] (NM)	−0.003(2)		3751(5)	29(4)	Abs.val.<10	
	Expt. [45] (GP)		66.1972(5)	3631.9(1)	31.472(1)		
	B3LYP-U	−0.0037	73.3	3700	27.6	−12.0	−0.3
	B3LYP-R	−0.0046	91.3	3460	16.6	−12.5	−0.6
	PBE0-U	−0.0045	90.2	3470	28.7	−8.8	−0.1
	PBE0-R	−0.0054	109	3220	16.3	−11.4	−0.5
$^{67}Zn^{1}H$	Expt. [46] (NM)	−0.0182(3)	$7.2(1)\times10^3$ (CA)	630(1)	15(1)	503(1)	−1(1)
	B3LYP-U	−0.0206	8.24×10^3	576	22.4	567	−0.2
	B3LYP-R	−0.0244	9.79×10^3	616	23.8	382	1.4
	PBE0-U	−0.0201	8.05×10^3	582	21.5	490	−0.5
	PBE0-R	−0.0240	9.60×10^3	606	23.0	348	1.4
$^{67}Zn^{19}F$	Expt. [47] (NM)	−0.006(1)	$1.3(2)\times10^2$ (CA)			319(2)	177(2)
	B3LYP-U	−0.0068	1.48×10^2	1230	13.4	305	252
	B3LYP-R	−0.0073	1.59×10^2	1160	15.4	266	210

TABLE IV. (*Continued*.)

Molecule (MX)	Source	$\Delta g_\perp$	γ (MHz)	$b_{F,M}$ (MHz)	t_M (MHz)	$b_{F,X}$ (MHz)	t_X (MHz)
	PBE0-U	−0.0071	1.55×10^2	1230	12.7	280	225
	PBE0-R	−0.0073	1.60×10^2	1140	14.7	259	190
$^{111}Cd^{19}F$	Expt. [47] (NM)	−0.017(2)	$4.8(6) \times 10^2$ (CA)			266(3)	202(2)
	B3LYP-U	−0.0271	7.60×10^2	−3590	−251	632	274
	B3LYP-R	−0.0314	8.79×10^2	−3600	−255	567	229
	PBE0-U	−0.0278	7.78×10^2	−3670	−240	582	252
	PBE0-R	−0.0320	8.96×10^2	−3630	−246	536	210
$^{67}Zn^{107}Ag$	Expt. [48] (AM)	−0.0118(2)	39(1) (CA)			−1324(3)*	0(1)
(optimized)	B3LYP-U	−0.0131	43.0	306	6.1	−1390	0.6
	B3LYP-R	−0.0158	52.0	306	6.9	−1250	−0.6
	PBE0-U	−0.0133	45.1	301	6.4	−1340	1.2
	PBE0-R	−0.0175	59.5	308	7.5	−1190	−0.5
$^{105}Pd^{1}H$	Expt. [49] (AM)	0.291(1)	$-1.252(4) \times 10^5$ (CA)	−823(4)	−22(3)		
	Expt. [49] (NM)	0.291(1)	$-1.252(4) \times 10^5$ (CA)	−857(4)	−16(3)		
	B3LYP-U	0.303	-1.30×10^5	−835	−13.5	93.3	8.4
	B3LYP-R	0.266	-1.14×10^5	−914	−2.4	117	7.0
	PBE0-U	0.285	-1.22×10^5	−801	−16.9	91.9	7.5
	PBE0-R	0.248	-1.07×10^5	−889	−4.2	125	6.6
$^{111}Cd^{1}H$	Expt. [50] (GP)	−0.0567(2) (CA)	$1.811(6) \times 10^4$	−3764(26)	−122(6)	558(10)	
	Expt. [51] (GP)			−3766.3(15)	−143(1)	549.8(18)	−2.4(8)
	B3LYP-U	−0.0597	1.95×10^4	−3510	−160	593	−0.6
	B3LYP-R	−0.0735	2.40×10^4	−3920	−175	374	0.9
	PBE0-U	−0.0586	1.91×10^4	−3620	−155	513	−0.9
	PBE0-R	−0.0724	2.36×10^4	−3950	−171	341	0.9
$^{111}Cd^{107}Ag$	Expt. [48] (AM)	−0.0312(2)	68.9(4)	−2053(3)*	−63(3)*	−1327(3)*	0(1)
	B3LYP-U	−0.0339	74.9	−1930	−47.7	−1370	−0.5
	B3LYP-R	−0.0400	88.4	−2010	−55.4	−1210	−0.6
	PBE0-U	−0.0355	80.4	−1910	−50.5	−1330	1.0
	PBE0-R	−0.0442	100	−2050	−60.6	−1150	−0.5
$^{7}Li^{40}Ca$	Expt. [52] (GP)	−0.0068(1) (CA)	103(2)				
	B3LYP-U	−0.0094	141	310	0.0	−95.0	−5.2
	B3LYP-R	−0.0119	179	218	0.2	−107	−4.6
	PBE0-U	−0.0090	134	260	−0.3	−85.1	−4.9
	PBE0-R	−0.0123	184	190	0.2	−104.4	−4.5
$^{7}Li^{138}Ba$	Expt. [53] (GP)	−0.1205(1) (CA)	1384.5(9)				
	B3LYP-U	0.854	−9820	172	−25.7	1010	−300
	B3LYP-R	−0.129	1480	162	0.3	806	28.1
	PBE0-U	−0.086	983	112	0.3	836	14.0
	PBE0-R	−0.134	1540	139	0.2	792	28.7
$^{40}Ca^{19}F$	Expt. [54] (GP)	−0.00193(1) (CA)	39.49793(2)			122.025(1)	13.549(1)
	B3LYP-U	−0.00195	39.8			126	8.2
	B3LYP-R	−0.00180	37.2			127	8.0
	PBE0-U	−0.02090	43.2			102	10.0
	PBE0-R	−0.00184	38.0			112	7.4
$^{88}Sr^{19}F$	Expt. [55] (GP)	−0.00495(1) (CA)	74.79485(10)			107.1724(10)	10.089(10)
	B3LYP-U	−0.00431	65.1			114	7.0
	B3LYP-R	−0.00463	69.9			112	6.8
	PBE0-U	−0.00469	65.1			90.8	8.1
	PBE0-R	−0.00485	73.2			98.5	6.1

form $F = 7/2$, $9/2$, and $11/2$. There are thus three zero-field states even for $N = 0$, spread over about 160 MHz by the coupling between i_{Sr} and S. For $N = 1$, these are each split into three by the spin-rotation coupling: $F = 7/2 \rightarrow \mathcal{F} = 5/2,7/2,9/2$; $F = 9/2 \rightarrow \mathcal{F} = 7/2,9/2,11/2$; $F = 11/2 \rightarrow \mathcal{F} = 9/2,11/2,13/2$. In a magnetic field these split into a total of $(2f_{Rb} + 1)(2i_{Sr} + 1)(2N + 1) = 90$ sublevels. The different angular momenta decouple sequentially as the magnetic field increases: first N, then i_{Sr}, and finally i_{Rb}. For $N > 0$ there are additional hyperfine couplings due to nuclear quadrupole interactions [$(eQq)_{Rb}$ and $(eQq)_{Sr}$] and anisotropic electron-nuclear spin couplings (t_{Rb} and t_{Sr}); these shift the resulting levels by a few MHz, but do not produce additional splittings. The resulting Zeeman diagram is very compli-

cated and is beyond the scope of this paper to explore in detail.

The situation is different again for CaF and SrF. Here the chemical interaction is strong enough that an atomic f quantum number for fluorine is not useful. The coupling between the electron and nuclear spins is much *smaller* than the separation between molecular rotational levels, so the ordering of levels is different. For even-mass Ca or Sr isotopes with $i = 0$, the primary coupling is between $S = 1/2$ and $i_F = 1/2$ to form $F = 0$ and 1. The resulting levels have been explored in previous work [54]. For ^{43}Ca and ^{87}Sr, however, the primary coupling is between $S = 1/2$ and $i_{Ca} = 7/2$ or $i_{Sr} = 9/2$. For ^{87}SrF these couple to form levels with $f_{Sr} = 4$ and 5, separated by about 2.6 GHz. These levels are then further split by weaker coupling to $i_F = 1/2$ to form zero-field $N = 0$ states $F = 7/2$, $9/2$, $9/2$, and $11/2$. For $N > 0$ these are further split by spin-rotation coupling. ^{43}CaF behaves analogously.

It is noteworthy that both the isotropic and dipolar magnetic hyperfine couplings are a factor of 7 to 10 stronger for ^{171}Yb in RbYb than for ^{87}Sr in RbSr. This makes ^{171}Yb a particularly appealing candidate for Feshbach resonances such as those predicted in Ref. [10] and observed for ^{87}Rb^{87}Sr in Ref. [11].

IV. CONCLUSIONS

Hyperfine coupling in $^2\Sigma$ molecules containing alkaline-earth-metal atoms is important both in producing ultracold molecules and in using them for applications in quantum science. We have used density-functional theory to calculate hyperfine coupling constants for several $^2\Sigma$ molecules that are the targets of current experiments aimed at producing ultracold molecules. We have focused on molecules formed from an alkaline-earth-metal (or Yb) atom and either an alkali-metal atom or fluorine. The resulting hyperfine splitting patterns and Zeeman splittings are illustrated by considering isotopologs of RbSr and SrF.

ACKNOWLEDGMENTS

This work was supported by the UK Engineering and Physical Sciences Research Council (EPSRC) Grants No. EP/H003363/1, No. EP/I012044/1, No. EP/P008275/1, and No. EP/P01058X/1. J.A. acknowledges funding by the Spanish Ministry of Science and Innovation Grants No. CTQ2012-37404-C02, No. CTQ2015-65033-P, and Consolider Ingenio 2010 CSD2009-00038.

APPENDIX

Table IV gives results for both spin-restricted and spin-unrestricted DFT calculations using the B3LYP [31] and PBE0 [32] functionals, for a variety of $^2\Sigma$ molecules for which experimental values are available. Overall, B3LYP is a little more accurate than PBEO and so we use B3LYP in the main paper. The largest fractional discrepancies are mostly in cases where the constants concerned are small and thus play a minor role for the molecule in question. In these cases the calculations correctly give small values, though sometimes with substantial percentage errors. For the remaining molecules, the spin-restricted results for $\Delta g_\perp$ (or equivalently γ) are accurate to 30% or better, with the exceptions of GaO and InO. The agreement is significantly better for b_F and t, except for InO. The exceptions probably arise because the ground states of these oxide radicals are mixtures of two electronic configurations with similar energies [33]. Molecular properties such as hyperfine coupling constants are very sensitive to the balance between the configurations.

Unrestricted calculations are often slightly more accurate than restricted calculations, especially for γ. However, in some cases they give very poor results, even where the fine and hyperfine coupling constants are large; see, for example, the values of b_F for the metals in AlO, GaO, and InO. It appears that unrestricted calculations on these oxides are even more susceptible to mixing of configurations than restricted calculations. The unrestricted B3LYP calculation also gives dramatically incorrect results for γ in LiBa: in this case we have calculated the effective spin of the molecule, and find that its value is far from $1/2$ in the unrestricted case, so it is clear that the solution suffers from spin contamination.

We conclude that spin-restricted B3LYP calculations give the most reliable overall results. It is, however, valuable to carry out unrestricted calculations as well: in cases where the two are similar, the unrestricted result may be better.

[1] K.-K. Ni, S. Ospelkaus, M. H. G. de Miranda, A. Pe'er, B. Neyenhuis, J. J. Zirbel, S. Kotochigova, P. S. Julienne, D. S. Jin, and J. Ye, Science **322**, 231 (2008).

[2] T. Takekoshi, L. Reichsöllner, A. Schindewolf, J. M. Hutson, C. R. Le Sueur, O. Dulieu, F. Ferlaino, R. Grimm, and H.-C. Nägerl, Phys. Rev. Lett. **113**, 205301 (2014).

[3] P. K. Molony, P. D. Gregory, Z. Ji, B. Lu, M. P. Köppinger, C. R. Le Sueur, C. L. Blackley, J. M. Hutson, and S. L. Cornish, Phys. Rev. Lett. **113**, 255301 (2014).

[4] J. W. Park, S. A. Will, and M. W. Zwierlein, Phys. Rev. Lett. **114**, 205302 (2015).

[5] M. Guo, B. Zhu, B. Lu, X. Ye, F. Wang, R. Vexiau, N. Bouloufa-Maafa, G. Quéméner, O. Dulieu, and D. Wang, Phys. Rev. Lett. **116**, 205303 (2016).

[6] A. Micheli, G. K. Brennen, and P. Zoller, Nat. Phys. **2**, 341 (2006).

[7] M. A. Baranov, M. Dalmonte, G. Pupillo, and P. Zoller, Chem. Rev. **112**, 5012 (2012).

[8] P. S. Żuchowski, J. Aldegunde, and J. M. Hutson, Phys. Rev. Lett. **105**, 153201 (2010).

[9] D. A. Brue and J. M. Hutson, Phys. Rev. A **87**, 052709 (2013).

[10] D. A. Brue and J. M. Hutson, Phys. Rev. Lett. **108**, 043201 (2012).

[11] V. Barbé, A. Ciamei, B. Pasquiou, L. Reichsöllner, F. Schreck, P. S. Żuchowski, and J. M. Hutson, arXiv:1710.03093.

[12] J. F. Barry, D. J. McCarron, E. B. Norrgard, M. H. Steinecker, and D. DeMille, Nature **512**, 286 (2014).

[13] S. Truppe, H. J. Williams, M. Hambach, L. Caldwell, N. J. Fitch, E. A. Hinds, B. E. Sauer, and M. R. Tarbutt, Nat. Phys. **13**, 1173 (2017).

[14] J. M. Brown and A. Carrington, *Rotational Spectroscopy of Diatomic Molecules* (Cambridge University, Cambridge, England, 2003).

[15] *Calculation of NMR and EPR Parameters: Theory and Applications,* edited by M. Kaupp, M. Bühl, and V. G. Malkin (Wiley-VCH Verlag, New York, 2004).

[16] R. A. Frosch and H. M. Foley, Phys. Rev. **88**, 1337 (1952).

[17] P. D. Gregory, J. A. Blackmore, J. Aldegunde, J. M. Hutson, and S. L. Cornish, Phys. Rev. A **96**, 021402(R) (2017).

[18] J. A. Blackmore, L. Caldwell, P. D. Gregory, E. M. Bridge, R. Sawant, J. Aldegunde, J. Mur-Petit, D. Jaksch, J. M. Hutson, B. E. Sauer, M. R. Tarbutt, and S. L. Cornish, arXiv:1804.02372.

[19] J. Aldegunde, B. A. Rivington, P. S. Żuchowski, and J. M. Hutson, Phys. Rev. A **78**, 033434 (2008).

[20] J. Aldegunde and J. M. Hutson, Phys. Rev. A **79**, 013401 (2009).

[21] J. Aldegunde, H. Ran, and J. M. Hutson, Phys. Rev. A **80**, 043410 (2009).

[22] J. Aldegunde and J. M. Hutson, Phys. Rev. A **96**, 042506 (2017).

[23] G. te Velde, F. M. Bickelhaupt, S. J. A. van Gisbergen, C. Fonseca Guerra, E. J. Baerends, J. G. Snijders, and T. Ziegler, J. Comput. Chem. **22**, 931 (2001).

[24] ADF2007.01, http://www.scm.com (2007), SCM, Theoretical Chemistry, Vrije Universiteit, Amsterdam, The Netherlands.

[25] E. van Lenthe, E. J. Baerends, and J. G. Snijders, J. Chem. Phys. **99**, 4597 (1993).

[26] E. van Lenthe, E. J. Baerends, and J. G. Snijders, J. Chem. Phys. **101**, 9783 (1994).

[27] E. van Lenthe, E. J. Baerends, and J. G. Snijders, J. Chem. Phys. **110**, 8943 (1999).

[28] R. F. Curl, Jr., Mol. Phys. **9**, 585 (1965).

[29] P. J. Bruna and F. Grein, Phys. Chem. Chem. Phys. **5**, 3140 (2003).

[30] W. Weltner, Jr., *Magnetic Atoms and Molecules* (Dover, New York, 1983).

[31] P. J. Stephens, F. J. Devlin, C. F. Chabalowski, and M. J. Frisch, J. Phys. Chem. **98**, 11623 (1994).

[32] J. Perdew, M. Ernzerhof, and K. Burke, J. Chem. Phys. **105**, 9982 (1996).

[33] L. B. Knight, T. J. Kirk, J. Herlong, J. G. Kaup, and E. R. Davidson, J. Chem. Phys. **107**, 7011 (1997).

[34] J. Fišer and R. Polák, Chem. Phys. **425**, 126 (2013).

[35] M. Pápai and G. Vankó, J. Chem. Theory Comput. **9**, 5004 (2013).

[36] P. Verma and J. Autschbach, J. Chem. Theory Comput. **9**, 1932 (2013).

[37] J. M. Brom, Jr., W. R. M. Graham, and W. Weltner, Jr., J. Chem. Phys. **57**, 4116 (1972).

[38] B. Kaving and R. Scullman, J. Mol. Spectrosc. **32**, 475 (1969).

[39] L. B. Knight, J. Herlong, T. J. Kirk, and C. A. Arrington, J. Chem. Phys. **96**, 5604 (1992).

[40] J. M. Brom and W. Weltner, J. Chem. Phys. **57**, 3379 (1972).

[41] P. Zeeman, Can. J. Phys. **29**, 336 (1951).

[42] C. Yamada, E. A. Cohen, M. Fujitake, and E. Hirota, J. Chem. Phys. **92**, 2146 (1990).

[43] L. B. Knight, J. G. Kaup, B. Petzoldt, R. Ayyad, T. K. Ghanty, and E. R. Davidson, J. Chem. Phys. **110**, 5658 (1999).

[44] W. Childs, O. Poulsen, and T. Steimle, J. Chem. Phys. **88**, 598 (1988).

[45] W. J. Childs, G. L. Goodman, L. S. Goodman, and L. Young, J. Mol. Spectrosc. **119**, 166 (1986).

[46] A. J. McKinley, E. Karakyriakos, L. B. Knight, R. Babb, and A. Williams, J. Phys. Chem. A **104**, 3528 (2000).

[47] L. B. Knight, Jr., A. Mouchet, W. T. Beaudry, and M. Duncan, J. Mag. Res. (1969) **32**, 383 (1978).

[48] P. H. Kasai and D. McLeod, Jr., J. Phys. Chem. **82**, 1554 (1978).

[49] L. B. Knight, S. T. Cobranchi, J. Herlong, T. Kirk, K. Balasubramanian, and K. K. Das, J. Chem. Phys. **92**, 2721 (1990).

[50] X. Q. Tan, T. M. Cerny, J. M. Williamson, and T. A. Miller, J. Chem. Phys. **101**, 6396 (1994).

[51] T. Varberg and J. Roberts, J. Mol. Spectrosc. **223**, 1 (2004).

[52] M. Ivanova, A. Stein, A. Pashov, A. V. Stolyarov, H. Knöckel, and E. Tiemann, J. Chem. Phys. **135**, 174303 (2011).

[53] J. D'Incan, C. Effantin, A. Bernard, G. Fabre, R. Stringat, A. Boulezhar, and J. Vergès, J. Chem. Phys. **100**, 945 (1994).

[54] W. J. Childs, G. L. Goodman, and L. S. Goodman, J. Mol. Spectrosc. **86**, 365 (1981).

[55] W. J. Childs, L. S. Goodman, and I. Renhorn, J. Mol. Spectrosc. **87**, 522 (1981).

[56] P. S. Żuchowski, R. Guérout, and O. Dulieu, Phys. Rev. A **90**, 012507 (2014).

[57] P. Colarusso, B. Guo, K.-Q. Zhang, and P. F. Bernath, J. Mol. Spectrosc. **175**, 158 (1996).

[58] M. L. Dubernet and J. M. Hutson, J. Chem. Phys. **99**, 7477 (1993).

[59] T. Takekoshi, M. Debatin, R. Rameshan, F. Ferlaino, R. Grimm, H.-C. Nägerl, C. R. Le Sueur, J. M. Hutson, P. S. Julienne, S. Kotochigova, and E. Tiemann, Phys. Rev. A **85**, 032506 (2012).

[60] M. Berninger, A. Zenesini, B. Huang, W. Harm, H.-C. Nägerl, F. Ferlaino, R. Grimm, P. S. Julienne, and J. M. Hutson, Phys. Rev. A **87**, 032517 (2013).